

END EFFECT IN LANGMUIR PROBE RESPONSE UNDER IONOSPHERIC SATELLITE CONDITIONS

Juan R. Sanmartin

April 1971

FLUID MECHANICS LABORATORY



DEPARTMENT OF MECHANICAL ENGINEERING
MASSACHUSETTS INSTITUTE OF TECHNOLOGY

D.D.C.
RECEIVED
MAY 27 1971
REGISTERED

47

Unclassified

Security Classification

DOCUMENT CONTROL DATA - R&D

(Security classification of title, body of abstract and indexing annotation must be entered when the overall report is classified)

1. ORIGINATING ACTIVITY (Corporate author) Massachusetts Institute of Technology Cambridge, Massachusetts 02139		2a. REPORT SECURITY CLASSIFICATION Unclassified	
		2b. GROUP	
3. REPORT TITLE End Effect in Langmuir Probe Response under Ionospheric Satellite Conditions			
4. DESCRIPTIVE NOTES (Type of report and inclusive dates)			
5. AUTHOR(S) (Last name, first name, initial) Sammartin, Juan R.			
6. REPORT DATE April 1971		7a. TOTAL NO. OF PAGES 36	7b. NO. OF REFS 6
8a. CONTRACT OR GRANT NO. N00014-0204-0040		8a. ORIGINATOR'S REPORT NUMBER(S) Fluid Mechanics Laboratory Publication No. 71-8	
b. PROJECT NO. c. d.		8b. OTHER REPORT NO(S) (Any other numbers that may be assigned this report)	
10. AVAILABILITY/LIMITATION NOTICES Distribution unlimited			
11. SUPPLEMENTARY NOTES		12. SPONSORING MILITARY ACTIVITY Advanced Research Projects Agency Department of Defense and Office of Naval Research, Washington, D.C.	
13. ABSTRACT A theory is presented for an end effect in the current response of a highly negative, cylindrical Langmuir probe in a collisionless plasma flow. Under conditions where ratio of probe radius to Debye length is small and the ion-acoustic Mach number is large, the current exhibits a strong peak when the probe axis is brought into alignment with the flow direction. Closed formulae are given for the maximum and angular half-width of the peak, and universal graphic results are presented for the entire peak structure. The theory shows very good agreement with experimental data. The use of the end effect for diagnostic purposes, in particular for the determination of the ion temperature, is discussed. ()			

14. KEY WORDS	LINK A		LINK B		LINK C	
	ROLE	WT	ROLE	WT	ROLE	WT
Langmuir probes						
Satellite instrumentation						
Ionospheric measurements						
Ion temperature measurement						

INSTRUCTIONS

1. **ORIGINATING ACTIVITY:** Enter the name and address of the contractor, subcontractor, grantee, Department of Defense activity or other organization (corporate author) issuing the report.

2a. **REPORT SECURITY CLASSIFICATION:** Enter the overall security classification of the report. Indicate whether "Restricted Data" is included. Marking is to be in accordance with appropriate security regulations.

2b. **GROUP:** Automatic downgrading is specified in DoD Directive 5200.10 and Armed Forces Industrial Manual. Enter the group number. Also, when applicable, show that optional markings have been used for Group 3 and Group 4 as authorized.

3. **REPORT TITLE:** Enter the complete report title in all capital letters. Titles in all cases should be unclassified. If a meaningful title cannot be selected without classification, show title classification in all capitals in parenthesis immediately following the title.

4. **DESCRIPTIVE NOTES:** If appropriate, enter the type of report, e.g., interim, progress, summary, annual, or final. Give the inclusive dates when a specific reporting period is covered.

5. **AUTHOR(S):** Enter the name(s) of author(s) as shown on or in the report. Enter last name, first name, middle initial. If military, show rank and branch of service. The name of the principal author is an absolute minimum requirement.

6. **REPORT DATE:** Enter the date of the report as day, month, year; or month, year. If more than one date appears on the report, use date of publication.

7a. **TOTAL NUMBER OF PAGES:** The total page count should follow normal pagination procedures, i.e., enter the number of pages containing information.

7b. **NUMBER OF REFERENCES:** Enter the total number of references cited in the report.

8a. **CONTRACT OR GRANT NUMBER:** If appropriate, enter the applicable number of the contract or grant under which the report was written.

8b, 8c, & 8d. **PROJECT NUMBER:** Enter the appropriate military department identification, such as project number, subproject number, system numbers, task number, etc.

9a. **ORIGINATOR'S REPORT NUMBER(S):** Enter the official report number by which the document will be identified and controlled by the originating activity. This number must be unique to this report.

9b. **OTHER REPORT NUMBER(S):** If the report has been assigned any other report numbers (either by the originator or by the sponsor), also enter this number(s).

10. **AVAILABILITY/LIMITATION NOTICES:** Enter any limitations on further dissemination of the report, other than those

imposed by security classification, using standard statements such as:

- (1) "Qualified requesters may obtain copies of this report from DDC."
- (2) "Foreign announcement and dissemination of this report by DDC is not authorized."
- (3) "U. S. Government agencies may obtain copies of this report directly from DDC. Other qualified DDC users shall request through _____."
- (4) "U. S. military agencies may obtain copies of this report directly from DDC. Other qualified users shall request through _____."
- (5) "All distribution of this report is controlled. Qualified DDC users shall request through _____."

If the report has been furnished to the Office of Technical Services, Department of Commerce, for sale to the public, indicate this fact and enter the price, if known.

11. **SUPPLEMENTARY NOTES:** Use for additional explanatory notes.

12. **SPONSORING MILITARY ACTIVITY:** Enter the name of the departmental project office or laboratory sponsoring (paying for) the research and development. Include address.

13. **ABSTRACT:** Enter an abstract giving a brief and factual summary of the document indicative of the report, even though it may also appear elsewhere in the body of the technical report. If additional space is required, a continuation sheet shall be attached.

It is highly desirable that the abstract of classified reports be unclassified. Each paragraph of the abstract shall end with an indication of the military security classification of the information in the paragraph, represented as (TS), (S), (C), or (U).

There is no limitation on the length of the abstract. However, the suggested length is from 150 to 225 words.

14. **KEY WORDS:** Key words are technically meaningful terms or short phrases that characterize a report and may be used as index entries for cataloging the report. Key words must be selected so that no security classification is required. Identifiers, such as equipment model designation, trade name, military project code name, geographic location, may be used as key words but will be followed by an indication of technical content. The assignment of links, rules, and weights is optional.

**END EFFECT IN LANGMUIR PROBE RESPONSE UNDER IONOSPHERIC
SATELLITE CONDITIONS**

by

Juan R. Sanmartin

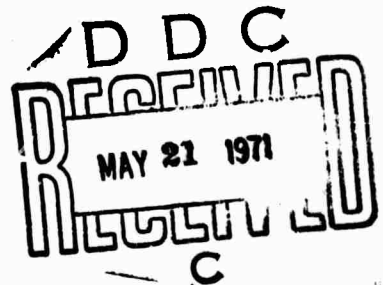
Fluid Mechanics Laboratory

**Department of Mechanical Engineering
Massachusetts Institute of Technology**

**This research was supported by the Advanced Research Projects
Agency of the Department of Defense and was monitored by the
Office of Naval Research under Contract No. N00014-0204-0040,
ARPA Order No. 322.**

**This document has been approved for public release and sale;
its distribution is unlimited.**

April 1971



END EFFECT IN LANGMUIR PROBE RESPONSE UNDER IONOSPHERIC
SATELLITE CONDITIONS

by

JUAN R. SANMARTIN

Department of Mechanical Engineering
Massachusetts Institute of Technology
Cambridge, Massachusetts

ABSTRACT

A theory is presented for an end effect in the current response of a highly negative, cylindrical Langmuir probe in a collisionless plasma flow. Under conditions where the ratio of probe radius to Debye length is small and the ion-acoustic Mach number is large, the current exhibits a strong peak when the probe axis is brought into alignment with the flow direction. Closed formulae are given for the maximum and angular half-width of the peak, and universal graphical results are presented for the entire peak structure. The theory shows very good agreement with experimental data. The use of the end effect for diagnostic purposes, in particular for the determination of the ion temperature, is discussed.

I - Introduction

The theory of an infinitely long, cylindrical Langmuir probe in a collisionless, quiescent plasma is particularly simple when the probe radius r_p is smaller than the Debye length λ_D , since then the current is "orbital motion limited"¹ and the old Langmuir analysis² is valid. Actually, that analysis is valid even in the more general case in which the plasma is in motion relative to the probe. If θ is the angle between probe axis and flow direction, and $-eV_p$ and $m_i U^2 \gg \kappa T_e, \kappa T_i$ (where V_p is the applied potential, κT_e is the electron thermal energy and κT_i and $m_i U^2$ are the ion thermal and directed energies, respectively) the current, J_∞ , to a probe of length l , as $l \rightarrow \infty$, is given by

$$J_\infty/l = 2N_0 eU \sin \theta r_p [1 - 2Z_i eV_p/m_i U^2 \sin^2 \theta]^{1/2} \quad (1)$$

where N_0 is the plasma density and Z_i is the ion charge number. Notice that according to Eq. (1) J_∞ decreases monotonically as θ goes from $\pi/2$ to zero.

In any actual experiment, however, l must be finite. Recently, probe current data have been reported from both satellite³ and laboratory⁴ experiments, for $r_p \ll \lambda_D$, $m_i U^2 \gg Z_i \kappa T_e$ and l/r_p as high as 820, that show a striking disagreement with J_∞ as given in Eq. (1). The current observed, J , was close to J_∞ as long as θ was not small, but as the probe approached the aligned orientation J exhibited a sharp

rise that peaked at $\theta = 0$ at a value many times larger than $J_{\infty}(\theta = 0)$. This phenomenon may be explained^{3,5} as an end effect due to the finite length of the probe. This shows that extremely long probes may be necessary if Eq. (1) is to be applicable in the interpretation of probe characteristics.

Of more interest for diagnostic purposes, however, is the end effect in itself. The peak may be quite strong, and should be possible to use it in the determination of the relative direction of the plasma flow, and of a number of plasma parameters. Of particular interest is the fact that both the height and the half-width of the peak are often sensitive to the ion temperature. This is very important because no other feature of probe response is known to be noticeably dependent on T_i .

Bettinger and Chen were the first authors to present a theoretical, although crude, analysis of the end effect; an important limitation of their approach, as pointed out in Ref. 5, was that l had to exceed a minimum value l_m [$l_m \approx 3\lambda_D (m_i U^2 / Z_i k T_e)^{1/2}$]. For $l < l_m$ some numerical computations were carried out by Hester and Sonin for $\theta = 0$.⁵

The present analysis starts from a similarity, suggested in Ref. 5, between the present steady-flow problem and a time-dependent one involving a quiescent plasma. In the next section the conditions for the validity of this Hester-Sonin (H-S) similarity are discussed in detail and the basic points of a theory⁶ recently developed for the time-dependent problem are introduced; this theory illustrates clearly

the anomalous behavior of the current as a function of θ . In Sec. III analytical and graphical results for the main features of the end effect are presented and compared with experimental data. The applications of the effect are discussed in Sec. IV, and Bettinger and Chen's analysis is discussed in an Appendix.

II - Basic Formulation

We consider a long, cylindrical Langmuir probe with length l and radius r_p in a collisionless plasma with unperturbed thermal energies κT_e and κT_i , density N_0 and bulk velocity relative to the probe U at an angle θ with its axis. The probe potential V_p is negative and such that

$$m_e U^2 \ll \kappa T_e \ll -eV_p ; \quad (2)$$

the electron current is then negligible and the perturbed electron density is given by Boltzmann's law

$$N_e = N_0 \exp(-\psi) \quad (3)$$

where $\psi \equiv -eV/\kappa T_e$ is the nondimensional potential field. Defining

$$\beta = T_i/Z_i T_e , \quad M = U/\lambda_D \omega_p , \quad (4)$$

$$\hat{l} = l/\lambda_D , \quad \epsilon = r_p/\lambda_D , \quad (5)$$

we assume that M and \hat{l} are large, ϵ small and $\beta \leq 1$; M is the ion-acoustic Mach number, $\lambda_D \equiv (\kappa T_e / 4\pi N_0 e^2)^{1/2}$ is the electron Debye length, $\omega_p \equiv (4\pi N_0 Z_1 e^2 / m_1)^{1/2}$ is the ion plasma frequency and m_1 and Z_1 are the ion mass and charge number. If $j(z)$ is the current density at the probe at distance z from its tip, the average current density

$$\bar{j} = \hat{l}^{-1} \int_0^{\hat{l}} j(z) dz$$

can then be written as a nondimensional function

$$\frac{\bar{j}}{j_\infty} = \frac{\bar{j}}{j_\infty}(\hat{l}, M, \epsilon, \beta, \psi_p, \theta) \quad (6)$$

where $j_\infty \equiv \bar{j}(\hat{l} \rightarrow \infty)$; according to Eq. (1)

$$j_\infty = \pi^{-1} N_0 e U \sin \theta [1 - 2Z_1 e V_p / m_1 U^2 \sin^2 \theta]^{1/2}. \quad (7)$$

The total current to the probe is $J = 2\pi r_p \hat{l} j_\infty$ times \bar{j}/j_∞ . To obtain this last quantity, the ion Vlasov equation must be solved together with Eq. (3) and Poisson's equation. The last one reads

$$\frac{1}{\rho} \frac{\partial}{\partial \rho} \rho \frac{\partial \psi}{\partial \rho} + \frac{1}{\rho^2} \frac{\partial^2 \psi}{\partial \phi^2} + \frac{\epsilon^2}{\hat{l}^2} \frac{\partial^2 \psi}{\partial \zeta^2} = \epsilon^2 v; \quad (8)$$

we have introduced cylindrical coordinates r, ϕ and z and have defined dimensionless quantities

$$\rho = r/r_p, \quad \zeta = z/l, \quad v_1 = (Z_1 N_1 - N_e)/N_0 \quad (9)$$

where N_1 is the perturbed ion density. ψ equals $\psi_p \equiv -eV_p/\kappa T_e$ at the probe and zero at infinity. The ion distribution function far ahead of the probe must also be known [even though $U \gg (\kappa T_1/m_1)^{1/2}$] and here will be assumed to be Maxwellian. [Thermal velocities may, and will, be neglected in the motion along the z-axis, but thermal motion in the $\rho - \phi$ plane is of fundamental importance when θ is small.]

Let us begin by considering the limit $\theta = 0$ (which also implies $\partial/\partial\phi = 0$). Hester and Sonin⁵ studied this limit and pointed out that, if \hat{l} and M^2/ψ_p are so large that $\partial^2\psi/\partial\zeta^2$ can be neglected in Eq. (8) and the ion velocity along the z-axis can be well approximated by its unperturbed value U , the steady flow problem is equivalent to a time-dependent one, wherein an infinitely long probe is immersed at time $t = 0$ in an unperturbed quiescent plasma, all other conditions being the same of the original problem. The time of flight of the ions down the probe z/U and the current density at z are respectively equivalent to the time t and the (spatially uniform) current density at t . As $z(t)$ increases, the ion distribution function readjusts itself and, if l is large enough, the "infinite" probe (steady state) limiting current density $j_\infty(\theta = 0)$ will eventually be reached. In the context of the time-dependent problem we can write

$$\frac{j}{j_\infty}(\theta = 0) = \frac{1}{t_l} \int_0^{t_l} \frac{j(t)}{j_\infty(\theta = 0)} dt \quad (10)$$

where

$$t_l = l/U \quad (11)$$

is the time equivalent of the length of the probe in the flowing plasma.

The time-dependent problem has been recently analyzed by Sanmartin⁶. His approach is based on the following points: (I) It is possible to derive an accurate expression for the electric field $\partial\psi/\partial\rho$ (for limited values of ρ) without solving simultaneously the ion Vlasov equation. Integrating Poisson's equation

$$\frac{1}{\rho} \frac{\partial}{\partial \rho} \rho \frac{\partial \psi}{\partial \rho} = \epsilon^2 v \quad (12)$$

yields a formal expression

$$\frac{\partial \psi}{\partial \rho} = - \frac{\psi_p \delta(t)}{\rho} + \frac{\epsilon^2}{2\rho} (\rho^2 - 1) \langle v(\rho, t) \rangle \quad (13)$$

where $-\psi_p \delta(t)$ is the field at the probe at time t and $\langle v \rangle$ is defined by

$$(\rho^2 - 1) \langle v(\rho, t) \rangle = \int_1^{\rho^2} d(\rho'^2) v(\rho', t) \quad (14)$$

$\delta(t)$ is found to change very little from $t = 0$ to $t = \infty$ so that an intermediate constant value $\bar{\delta}$ can be used in Eq. (13); one finds

$$\bar{\delta}^{-1} = \ln \epsilon^{-1} + Y(\epsilon, \psi_p) \quad (15)$$

where Y is given in Fig. 1. $\langle v \rangle$ varies over the entire range $1 \geq \langle v \rangle \geq 0$; however, in a certain neighborhood of the probe, roughly $\rho \leq \rho_m \equiv (2\psi_p \bar{\delta})^{1/2} \epsilon^{-1}$, $\langle v \rangle$ is found to change very slowly and to have a central value \bar{v} that is approximately 0.80. For details on these results and their accuracy, see Ref. 6. Thus, for $\rho \leq \rho_m$, the electric field may be correctly approximated by a function that only depends on ρ

$$\frac{\partial \psi}{\partial \rho} = -\frac{\psi_p \bar{\delta}}{\rho} + \frac{\epsilon^2 \bar{v}}{2\rho} (\rho^2 - 1) \quad (16)$$

Although for ϵ small the concept of a sheath has little meaning ("orbital motion limited" current implies an infinite sheath in the Langmuir sense²) both ρ_m and $\exp(\bar{\delta}^{-1})$, which are close to each other, may be thought of as characteristic sheath radii. If t_m is the typical time of flight to the probe of ions that were at the boundary of that sheath at $t = 0$, it is clear that the theory is only valid for, roughly, $t \leq t_m$.

(II) With the field known, ion trajectories may be computed explicitly. Moreover, the current to the probe is linear in the (unperturbed) ion distribution function at $t = 0$, $f_0(\vec{v}_\perp^*)$. It suffices therefore to determine the current for the simplest possible f_0 , that for which all ions have velocities of the same magnitude v_\perp^* and direction (parallel to an arbitrarily chosen polar axis); see Fig. 2. Once that current, $\bar{j}^*(v_\perp^*)/j_\infty$, has been found, the current for any

other f_0 is given by a definite integral, $\int f_0(\vec{v}_1^*) d\vec{v}_1^* \bar{j}^*(v_1^*)/j_\infty$. To find \bar{j}^*/j_∞ one can use energy and angular momentum conservation to divide the $\rho - \phi$ plane at $t = 0$ in two mutually exclusive regions $A^*(v_1^*)$ and $B^*(v_1^*)$: a point $\rho - \phi$ belongs to A^* if an ion having such initial coordinates, and moving under the field given by Eq. (16), will strike the probe at some $t > 0$. The time of flight to the probe of every point in A^* can be computed and, therefore, a function $a^*(v_1^*, t)$ can be determined which represents the area of that part of A^* which has been "collected" by the time t . The current per unit length of probe is then

$$2\pi r_p j^*(t) = N_0 e da^*/dt \quad (17)$$

and defining $a(t) = \int a^* d\vec{v}_1^* f_0(\vec{v}_1^*)$, we have

$$2\pi r_p j(t) = N_0 e da/dt \quad (18)$$

The average value of j is

$$\bar{j} = \frac{N_0 e}{2\pi r_p} \frac{a(t)}{t} \quad (19)$$

and in nondimensional form

$$\frac{\bar{j}}{j_\infty} = \frac{\epsilon \hat{a}(\tau)}{(8\psi_p)^{1/2} \tau} \quad (20)$$

where $\tau = \omega_p t$ and \hat{a} is a nondimensional form of the area, $\hat{a} = a/r_p^2$.

The general behavior of \bar{j}/j_∞ can be determined by a qualitative discussion of \bar{j}^*/j_∞ assuming that v_1^* is of the order of the characteristic ion velocity. The condition for a point $\rho_0 - \phi_0$ to belong to A^* follows from the equations of motion of an ion with initial coordinates $\rho_0 - \phi_0$. One finds

$$|\sin \phi_0| \leq G(\rho_0)/\rho_0, \quad (21)$$

$$G \equiv [1 + \ln \rho_0^2/\alpha^* - \bar{v} (\rho_0^2 - 1)/\alpha^* \rho_m^2]^{1/2}$$

where

$$\alpha^* = \frac{2\beta^*}{\psi_p \delta}, \quad \beta^* = \frac{m_1 (v_1^*)^2}{2Z_1 \kappa T_e}. \quad (22)$$

For $\psi_p \gg 1$, $\beta^* \leq 1$, as assumed here, we have $\alpha^* \ll 1$. For all $\alpha^* < 1$ there is a value ρ_q such that $G(\rho_q)/\rho_q = 1$ and then $G(\rho_0)/\rho_0 > 1$ for $\rho_0 < \rho_q$. $\bar{\rho}_A(\phi)$, the boundary of A^* given by Eq. (21), has the form indicated in Fig. 2.⁷ As the ion temperature increases, α^* goes up and point q moves down reaching $\rho = 1$ at $\alpha^* = 1$; for $\alpha^* > 1$, we have $G(\rho_0)/\rho_0 \leq 1$ for all $\rho_0 \geq 1$. Now, $\partial\psi/\partial\rho \sim \rho^{-1}$ for, say, $\rho < \rho_m/3$ [see Eq. (16)] and the potential field is then logarithmic. The mean velocity of an ion with ρ_0 in that region, in its trip to the probe, is nearly independent of ρ_0 ; specifically $\rho_0/\tau_0 \sim \rho_m$, where $\tau_0(\rho_0, \phi_0)$ is the time of flight to the probe.

Therefore, as long as $\rho_0 < \rho_q$,

$$\hat{a}^* \sim \rho_m^2 \tau^2 \sim \psi_p \bar{\delta} \tau^2 / \epsilon^2 \quad (23)$$

and

$$\bar{j}^*/j_\infty \sim \epsilon \hat{a}^* / \tau \psi_p^{1/2} \sim \psi_p^{1/2} \bar{\delta} / \epsilon \quad (24)$$

\bar{j}^*/j_∞ grows linearly with τ until $\tau = \tau_q \equiv \tau_0(\rho_0 = \rho_q, \phi_0 = \pi/2)$, when \hat{a}^* switches from a quadratic growth in ρ_0 to a nearly linear one; for even larger τ , \bar{j}^*/j_∞ will actually decline because ions from outside the $\partial\psi/\partial\rho \sim \rho^{-1}$ region will begin to be collected and both field and ion mean velocity, ρ_0/τ_0 , will rapidly decrease. Neglecting logarithmic variations we get, from (21),

$$\rho_q \sim (\psi_p \bar{\delta} / \beta^*)^{1/2} \quad (25)$$

so that putting $\tau = \tau_q \sim \rho_q / \rho_m$ in (24) we obtain the peak in \bar{j}^*/j_∞ ,

$$\bar{j}^*/j_\infty \sim (\psi_p / \beta^*)^{1/2} \bar{\delta} \quad (26)$$

which can be far greater than unity and depends on β^* . The overshoot represented by (26) may be seen as caused by the sudden set-up of the potential field which traps low angular momentum ions in the neighborhood of the probe; when β^* decreases, ρ_q increases and the low angular

momentum region increases too. Eventually, however, a value of β^* is reached for which ρ_q moves out of the $\partial\psi/\partial\rho \sim \rho^{-1}$ region; the growth of \bar{j}^*/j_∞ , as given in (24), is then stopped by the rapidly decreasing value of ρ_0/τ_0 , and not by the fact that the boundary of A^* has been reached. The effect is the same for all smaller β^* so that the current is now insensitive to the actual value of β^* . The critical value of β^* is found by putting $\rho_q \sim \rho_m$, i.e. $\tau_q \sim 1$,

$$\beta^* \sim \epsilon^2 ; \quad (27)$$

the maximum current peak possible is

$$\bar{j}^*/j_\infty \sim \psi_p^{1/2} \bar{\delta}/\epsilon . \quad (28)$$

According to the H-S similarity, the functions given in Eqs. (20) and (6) (for $\theta = 0$) are the same. Equation (20) depends on τ , ϵ , β and ψ_p . In the flow problem the value corresponding to τ is $\tau_\ell \equiv \omega_p t_\ell = \hat{\ell}/M$; the parameters $\hat{\ell}$ and M in Eq. (6) appear, therefore, combined in a single one. All the qualitative results derived above for \bar{j}/j_∞ need not be repeated and we shall only add two new points.

(1) For the present problem, Eqs. (19) and (20) become

$$\bar{j} = \frac{N_0 e U a(\ell/U)}{2\pi r_p \ell} , \quad (29)$$

$$\frac{\bar{j}}{j_\infty} = \frac{\epsilon M}{(8\psi_p)^{1/2} \hat{\ell}} \hat{a}(\hat{\ell}/M) . \quad (30)$$

Equation (19) makes clear the meaning of $a(l/U)$: The total current to the probe is

$$J = 2\pi r_p l \bar{j} = N_0 e U a(l/U) \quad (31)$$

so that $a(l/U)$ is an effective probe cross section in the plane perpendicular to the flow. (2) As already indicated, the analysis of Ref. 6 is only valid for $t < t_m$; one finds that $\tau_m \equiv \omega_p t_m \approx 3$. Thus the results of the present paper will be valid for, roughly,

$$\hat{l} < 3M \quad (32)$$

We note that the peak in \bar{j}/j_∞ occurs at $\tau \approx 1$.

The theory given above explains the large value of \bar{j}/j_∞ at $\theta = 0$. It can also explain its sharp decrease when the probe is turned by a small angle. For $\theta \neq 0$ the problem changes in three respects. First, the unperturbed distribution function in the $\rho - \phi$ plane, $f_0(\vec{v}_\perp^*)$, has now a drift velocity $U \sin \theta$; second, the Laplacian in Poisson's equation includes the term $\rho^{-2} \partial^2 \psi / \partial \phi^2$; finally, angular momentum is not conserved. We shall now assume that the last two changes have no substantial effect on the current to the probe; this point is discussed in the Appendix. Then the results for $\bar{j}^*(v_\perp^*)/j_\infty$, v_\perp^* arbitrary, are not changed; the drift is taken into account by using the new form of $f_0(\vec{v}_\perp^*)$, which now has two characteristic velocities, $(\kappa T_1/m_1)^{1/2}$ and

$U \sin \theta$. It is clear therefore that Eq. (6) may be written as

$$\frac{\bar{j}}{j_\infty} = \frac{\bar{j}}{j_\infty} \left(\frac{\hat{l}}{M \cos \theta}, \epsilon, \mu, \frac{M^2 \sin^2 \theta}{2}, \psi_p \right) \quad (33)$$

Now the characteristic values of β^* and α^* to be used in our earlier discussion on \bar{j}^*/j_∞ are not $\beta^* \sim \beta$ and $\alpha^* \sim 2\beta/\psi_p \bar{\delta}$ but, say,

$$\beta^* \approx \beta + \frac{M^2 \sin^2 \theta}{2} \equiv \beta_T, \quad (34)$$

$$\alpha^* \approx \frac{2}{\psi_p \bar{\delta}} \left(\beta + \frac{M^2 \sin^2 \theta}{2} \right) \equiv \alpha_T \quad (35)$$

(although the effects of β and $M^2 \sin^2 \theta/2$ in (33) are not exactly additive, they may be considered so in a qualitative discussion). As long as θ is so small that $\beta_T \approx \beta$, the current remains fairly constant. When θ becomes of the order of $(2\beta)^{1/2}/M$ or $(2\epsilon^2)^{1/2}/M$, whatever the largest, the current begins to decrease. When θ is so large that $\alpha_T \gg 1$, we have $\rho_q \leq 1$ and so $G(\rho_0)/\rho_0$ in Eq. (21) is always less than one. Thus $\hat{\alpha}^*$ always grows (almost) linearly in ρ_0 , while ρ_0/τ_0 remains fairly constant. Therefore $\bar{j}^*/j_\infty \approx 1$ (except for $\hat{l}/M \cos \theta$ very small). We note that in fact the peak in the current disappears for θ smaller than the value for which $\alpha_T = 1$.

Before using the results of the preceding time-dependent theory in the flow problem, we must examine more carefully the assumptions

behind the H-S similarity. First, if the $\partial^2 \psi / \partial \zeta^2$ term is retained in Poisson's equation, Eq. (13) would read

$$\frac{\partial \psi}{\partial \rho} = \frac{-\psi_p \delta(\zeta)}{\rho} + \frac{\epsilon^2}{2\rho} \langle v(\rho, \zeta) - \hat{\ell}^{-2} \frac{\partial^2 \psi}{\partial \zeta^2} \rangle (\rho^2 - 1) \quad (36)$$

where $\langle \rangle$ has the same meaning of Eq. (14) and we have used the variable ζ equivalent to τ . We want to find out some quantitative condition for writing

$$\langle v - \hat{\ell}^{-2} \partial^2 \psi / \partial \zeta^2 \rangle \approx \langle v \rangle \quad (37)$$

in Eq. (36). The equation itself can be used to obtain $\partial^2 \psi / \partial \zeta^2$ by integrating once with respect to ρ and deriving twice with respect to ζ . If (37) is valid we get

$$\begin{aligned} \hat{\ell}^{-2} \frac{\partial^2 \psi}{\partial \zeta^2} &= \frac{\psi_p \delta}{2\hat{\ell}^2} [2\delta \ln \rho \{ \frac{d^2 \delta^{-1}}{d\zeta^2} - 2\delta (\frac{d\delta^{-1}}{d\zeta})^2 \} \\ &+ \frac{\bar{\delta}}{\delta} \int_1^{\rho} 2 \frac{(\rho' - 1/\rho')}{\rho_m^2} d\rho' \langle \frac{\partial^2 v}{\partial \zeta^2} \rangle] \end{aligned}$$

so that

$$\begin{aligned} \langle v - \hat{\ell}^{-2} \frac{\partial^2 \psi}{\partial \zeta^2} \rangle &\approx \bar{v} - \frac{\psi_p \bar{\delta}}{2\hat{\ell}^2} [\bar{\delta} (2 \ln \rho - 1) \langle \frac{d^2 \delta^{-1}}{d\zeta^2} - 2\bar{\delta} (\frac{d\delta^{-1}}{d\zeta})^2 \rangle \\ &+ \frac{\rho^2}{2\rho_m^2} \langle \frac{\partial^2 v}{\partial \zeta^2} \rangle] \end{aligned}$$

Both $(2 \ln \rho - 1)$ and ρ^2 have maxima at the largest value of ρ considered; thus we have

$$\langle v - \hat{\ell}^{-2} \frac{\partial^2 \psi}{\partial \zeta^2} \rangle_{\rho \rho_m} \approx \bar{v} - \frac{\psi_p \bar{\delta}}{2 \hat{\ell}^2} \approx 2 \frac{d^2 \delta^{-1}}{d \zeta^2} - 4 \bar{\delta} \left(\frac{d \delta^{-1}}{d \zeta} \right)^2 + \frac{1}{2} \frac{\partial^2 v}{d \zeta^2}.$$

We estimate $d \delta^{-1} / d \zeta \approx \Delta \delta^{-1} / \Delta \zeta < \delta^{-1}(\zeta = \infty) - \delta^{-1}(\zeta = 0)$, $d^2 \delta^{-1} / d \zeta^2 \approx 2 \Delta \delta^{-1}$, $\partial^2 v / \partial \zeta^2 \approx 2 \Delta v$. For the typical values of ϵ and ψ_p to be later considered, $\delta^{-1}(\zeta = \infty) - \delta^{-1}(\zeta = 0) \approx 0.15$ and $\Delta v < 0.20$. Thus we obtain

$$\langle v - \hat{\ell}^{-2} \frac{\partial^2 \psi}{\partial \zeta^2} \rangle_{\rho \rho_m} \approx \bar{v} - \frac{4 \psi_p \bar{\delta}}{\hat{\ell}^2} \approx 0.1. \quad (38)$$

Since $4 \bar{\delta}$ is never far from unity and the absolute error in writing $\langle v \rangle = \bar{v}$ is typically 0.1 we find that the condition for the neglect of $\partial^2 \psi / \partial \zeta^2$ in Poisson's equation is roughly

$$\hat{\ell} > \psi_p^{1/2}. \quad (39)$$

Second, if the z-equation of motion of an ion is twice integrated up to $z = \ell$, with initial conditions $z = 0$ and $dz/dt = U$, we get an equation for the time t_ℓ that the ion takes to travel the probe

$$1 = \frac{U t_\ell}{\ell} \left[1 + \frac{U t_\ell}{\ell} \frac{\bar{\psi}_\zeta}{2 M^2} \right] \quad (40)$$

where $\bar{\psi}_\zeta$ is given by

$$t_{\ell}^2 \bar{\psi}_{\zeta} = 2 \int_0^{t_{\ell}} (t_{\ell} - t) dt \partial\psi/\partial\zeta \quad (41)$$

and this integral is along the trajectory of the ion. If $\partial\psi/\partial\zeta$ is small enough, the bracket in Eq. (40) becomes unity and we get the uniform motion assumption, $t_{\ell} = \ell/U$, on which the H-S similarity is based. This can only be true if $\bar{\psi}_{\zeta}/2M^2$ is very small. Integrating Eq. (36) with respect to ρ and deriving with respect to ζ we get

$$\frac{\partial\psi}{\partial\zeta} = \psi_p \ln \rho \delta^2 \frac{d\delta^{-1}}{d\zeta} + \epsilon^2 \int_1^{\rho} \frac{\rho'^2 - 1}{2\rho'} d\rho' \left\langle \frac{\partial v}{\partial\zeta} \right\rangle \quad (42)$$

so that, at most,

$$\frac{\bar{\psi}_{\zeta}}{2M^2} \approx 0.4 \frac{\bar{\delta} \psi_p}{4M^2} \quad (43)$$

where we considered the worst possible case (initial ρ equal to ρ_m) and estimated $d\delta^{-1}/d\zeta \approx 0.15$, $\partial v/\partial\zeta \approx 0.20$. From Eq. (43) we conclude that if

$$\psi_p < M^2, \quad (44)$$

we have $t_{\ell} = \ell/U$ with an error of 3% or less.

Third, we note that (1) to actually obtain the current to the probe we must add to Eq. (31) the expression $N_0 e U \pi r_p^2$ [the front end of the probe was excluded from a (ℓ/U)], and (2) Sanmartin's analysis

concerned a probe whose potential was switched from zero to V_p at $t = 0$ (instead of a probe suddenly immersed in a plasma). The corrections resulting from points (1) and (2) are only important if $\tau_l \ll 1$, but will be incorporated into the results in the next section.

III - The Ion Current

An expression for \bar{j}^*/j_∞ was obtained in Ref. 6. Neglecting some terms that amount to less than 2% and taking into account the corrections indicated in the last paragraph of Sec. II, we get (for $\tau = \tau_l$)

$$\frac{\bar{j}^*}{j_\infty} = \frac{\epsilon}{(8\psi_p)^{1/2} \tau_l} \pi \sigma^2 \quad \alpha^* < h, \quad (45)$$

$$= \frac{\epsilon}{(8\psi_p)^{1/2} \tau_l} \pi \sigma^2 \left[\frac{2}{\pi} \left\{ \sin^{-1} \left(\frac{h}{\alpha^*} \right)^{1/2} + \frac{(\alpha^*/h - 1)^{1/2}}{\alpha^*/h} \right\} \right]$$

$$+ \frac{h}{\alpha^*} 2 \frac{1 - \sigma^{-2}}{\ln \sigma^2} \left\{ 1 - \frac{2}{\pi} \sin^{-1} \left(\frac{h}{\alpha^*} \right)^{1/2} - \frac{2}{\pi} \left(\frac{\alpha^*}{h} - 1 \right)^{1/2} \right\}$$

$$\alpha^* > h, \quad (46)$$

where σ is given by

$$\sigma \operatorname{Erf}(\ln \sigma)^{1/2} = (2\psi_p \bar{\delta})^{1/2} F(\tau_l)/\epsilon \quad (47)$$

and

$$h = \ln \sigma^2 / (\sigma^2 - 1) , \quad (48)$$

$$F(\tau_L) = \tau_L (\pi + 0.6 \tau_L^2)^{-1/2} . \quad (49)$$

The actual nondimensional ion current \bar{j}/j_∞ may be obtained from

$$\bar{j}/j_\infty = \int d\vec{v}_1^* f_0(\vec{v}_1^*) \bar{j}^*/j_\infty . \quad (50)$$

The unperturbed ion distribution function in the plane $z = 0$ is Maxwellian with a drift $U \sin \theta$ so that from Eq. (50) we get

$$\begin{aligned} \frac{\bar{j}}{j_\infty} &= \int_0^{2\pi} d\gamma \int_0^\infty v_1^* dv_1^* \frac{m_1}{2\pi k T_1} \exp \left[-\frac{m_1}{2k T_1} \{ (v_1^*)^2 + U^2 \sin^2 \theta \right. \\ &\quad \left. - 2v_1^* U \sin \theta \cos \gamma \} \right] \bar{j}^*/j_\infty \\ &= \int_0^\infty \frac{dv}{\eta} \exp \left(-\frac{v}{\eta} \right) \exp \left(-\frac{\mu^2}{\eta} \right) I_0 \left(2 \frac{\mu}{\eta} v^{1/2} \right) \frac{\bar{j}^*}{j_\infty} \end{aligned} \quad (51)$$

where

$$\eta = 2B/\psi_p \bar{\delta} h , \quad \mu^2 = M^2 \sin^2 \theta / \psi_p \bar{\delta} h . \quad (52)$$

Using Eqs. (45) and (46) we can write (51) as

$$\frac{\bar{j}}{j_\infty} = \frac{\pi \epsilon \sigma^2}{(8\psi_p)^{1/2} \tau_\ell} [X_0(\mu, \eta) + sX_1(\mu, \eta)] \quad (53)$$

where

$$s = 2(1 - \sigma^{-2})/\ln \sigma^2$$

and

$$\begin{aligned} X_0(\mu, \eta) \equiv X_0^{\mu\eta} &= \eta^{-1} \exp(-\mu^2/\eta) \int_0^1 dv \exp(-v/\eta) I_0(2\mu v^{1/2}/\eta) \\ &+ \eta^{-1} \exp(-\frac{\mu^2}{\eta}) \int_1^\infty dv \exp(-\frac{v}{\eta}) I_0(2\mu \frac{v^{1/2}}{\eta}) \frac{2}{\pi} \left[\sin^{-1} \frac{1}{v^{1/2}} + \frac{(v-1)^{1/2}}{v} \right], \end{aligned} \quad (54)$$

$$\begin{aligned} X_1(\mu, \eta) \equiv X_1^{\mu\eta} &= \eta^{-1} \exp(-\frac{\mu^2}{\eta}) \int_1^\infty dv \exp(-\frac{v}{\eta}) I_0(2\mu v^{1/2}/\eta) \\ &\cdot \frac{1}{v} \left[1 - \frac{2}{\pi} \sin^{-1} \frac{1}{v^{1/2}} - \frac{2}{\pi} (v-1)^{1/2} \right]. \end{aligned} \quad (55)$$

It has not been possible to carry out the integrations in (54) and (55) analytically. A number of limiting expressions may be easily derived, however. For $\eta \rightarrow 0$ (cold ions limit) we get

$$\begin{aligned} X_0^{\mu 0} + sX_1^{\mu 0} &= 1, \quad \mu \leq 1 \\ &= \frac{2}{\pi} \left[\sin^{-1} \frac{1}{\mu} + \frac{(\mu^2 - 1)^{1/2}}{\mu} \right] + \frac{s}{\mu^2} \\ &\cdot \left[1 - \frac{2}{\pi} \sin^{-1} \frac{1}{\mu} - \frac{2}{\pi} (\mu^2 - 1)^{1/2} \right] \quad \mu \geq 1. \end{aligned} \quad (56)$$

For $\mu \rightarrow 0$,

$$x_0^{0\eta} + s x_1^{0\eta} = \text{Erf } \eta^{-1/2} + 2(\pi\eta)^{-1/2} \exp(-\eta^{-1}) - 2\eta^{-1} \text{Erfc } \eta^{-1/2} \\ + s[\eta^{-1} E_1(2\eta^{-1}) - 2(\pi\eta)^{-1/2} \exp(-\eta^{-1}) \text{Erfc } \eta^{-1/2}] \quad (57)$$

For η fixed and $\mu \rightarrow \infty$

$$x_0^{\mu\eta} + s x_1^{\mu\eta} \approx x_0^{\mu 0} + s x_1^{\mu 0} \approx \frac{4}{\pi\mu} - s \frac{2}{\pi\mu} \quad ; \quad (58)$$

all curves approach the cold ion limit. Finally for μ^2/η fixed and $\eta \rightarrow \infty$

$$x_0^{\mu\eta} + s x_1^{\mu\eta} \approx \frac{4}{(\pi\eta)^{1/2}} \exp\left(-\frac{\mu^2}{2\eta}\right) I_0\left(\frac{\mu^2}{2\eta}\right) \left(1 - \frac{s}{2}\right) \quad ; \quad (59)$$

as $\mu^2/2\eta \rightarrow 0$ this equation approaches $4(\pi\eta)^{-1/2} (1 - s/2)$, which is the limit of Eq. (57) as $\eta \rightarrow \infty$. Equation (59) can be also rewritten as

$$x_0^{\mu\eta} + s x_1^{\mu\eta} \approx \frac{4}{\pi\mu} \left(\frac{\mu^2}{2\eta}\right)^{1/2} \exp\left(-\frac{\mu^2}{2\eta}\right) I_0\left(\frac{\mu^2}{2\eta}\right) (2\pi)^{1/2} \left(1 - \frac{s}{2}\right) \quad ; \quad (60)$$

as $\mu^2/2\eta \rightarrow \infty$, Eq. (60) approaches $4(1 - s/2)/\pi\mu$, which is the limit of Eq. (56) as $\mu \rightarrow \infty$.

$X \equiv X_0 + sX_1$ is given graphically in Fig. 3 as a function of μ for several values of η . For each η , curves for two values of s have been represented ($s = 0, s = 1/3$); interpolation and extrapolation for different s are immediate because X is linear in s . We note that X is practically always very close to X_0 . The function $X(\mu)$ is a direct representation of the peak structure, since $X \sim \bar{j}/j_\infty$ and $\mu \sim \theta$.

In the computation of X an overshoot was observed for the largest values of η in Fig. 3: in approaching the cold ions ($\eta = 0$) curve, each (large) $\eta = \text{constant}$ curve overshoot it and then approached it from above. This effect was so small that it could not show up clearly in the figure, and all curves were interrupted when first meeting the $\eta = 0$ curve. The existence of the overshoot may be seen explicitly in Eq. (60), valid for large η , since the function

$$(2\pi y)^{1/2} \exp(-y) I_0(y) ,$$

which is zero at $y = 0$ and unity at $y = \infty$, has a maximum 1.17, at $y \approx 0.80$. Actually, this would indicate that the overshoot should be substantial; thus, one may conclude that for the moderately large values of η here considered, finite η effects partially mask the overshoot.

The fact that the $\eta = 0$ curve is not an upper bound of the family $\eta = \text{constant}$ implies that the seemingly obvious condition $\partial X / \partial \eta < 0$

is violated for some values of η and μ . That this is possible may be easily understood by noticing that if \vec{v}_1^* is the vectorial composition of an equiprobably oriented (thermal) velocity and a directed velocity (the drift) forming an angle γ with each other, an increment of either component may decrease the value of v_1^* for a certain range of values of γ ; under some conditions the increase in current in this range may dominate the decrease that appears at all other values of γ .

From Eqs. (56) and (57), closed formulae may be derived for the main features of the current peak, that is, its maximum and its angular half-width $\hat{\theta}_{1/2}$ (the width of the peak at half-value of its maximum). For the maximum we have

$$\left. \frac{j}{j_\infty} \right|_{\max} = \frac{j}{j_\infty} (\theta = 0) = \frac{\pi \epsilon \sigma^2 M}{(8\psi_p)^{1/2} \hat{i}} [x_0^{0\eta} + s x_1^{0\eta}] ; \quad (61)$$

the functions $x_0^{0\eta}$ and $x_1^{0\eta}$, given in Eq. (57), are graphically represented in Fig. 4 for convenience. For the half-width we have the condition

$$x_0^{\mu\eta} + s x_1^{\mu\eta} = 0.5 [x_0^{0\eta} + s x_1^{0\eta}] , \quad (62)$$

where, from Eq. (52),

$$\mu = \hat{\mu}_{1/2} \equiv \frac{M \hat{\theta}_{1/2} (\sigma^2 - 1)^{1/2}}{2(\psi_p \delta \ln \sigma^2)^{1/2}} . \quad (63)$$

We now note that all curves in Fig. 3 meet the cold-ions limiting curve at values of μ clearly smaller than $\hat{\mu}_{1/2}$. Thus we can rewrite Eq. (62) as

$$x_0^{\mu 0} + s x_1^{\mu 0} = 0.5 [x_0^{0\eta} + s x_1^{0\eta}] \quad ; \quad (64)$$

this equation only involves the functions given in Eqs. (56) and (57). A useful, explicit approximation for $\hat{\theta}_{1/2}$ may be obtained by neglecting the dependence on s and writing

$$x_0^{\mu 0} \approx 4/\pi [\mu^2 + (4/\pi)^2 - 1]^{-1/2}$$

which has an error of less than 3%; we then have

$$\hat{\theta}_{1/2} \approx 2 \left[\frac{\psi_p \bar{\delta} \ln \sigma^2}{M^2 (\sigma^2 - 1)} \right]^{1/2} \left[\left(\frac{8}{\pi x_0^{0\eta}} \right)^2 + 1 - \left(\frac{4}{\pi} \right)^2 \right]^{1/2} \quad . \quad (65)$$

Equation (64) has been solved exactly for $s = 0$ and $s = 1/3$; $\hat{\mu}_{1/2}(\eta)$ is given graphically in Fig. 5.

Figure 6 presents $\bar{j}/j_\infty \big|_{\max}$ versus \hat{l}/M for a fixed ψ_p and several values of ϵ , from both Eq. (61) and the experimental data discussed in Ref. 6. Theoretical curves are presented for both $\beta = 10^{-2}$ (full line) and $\beta = 10^{-3}$ (dashed line). In Ref. 6 it was estimated that in the experiments β was of order 10^{-2} or less, and it was assumed

that a cold ion theory would, therefore, apply. Our analysis shows that the condition for a cold ion theory is not $\beta \ll 1$ but $\eta \ll 1$ (or more weakly, $\eta < 0.5$, say); this shows up clearly in Fig. 6 for the largest values of ϵ^{-1} and \hat{l}/M . The agreement with the experiments is excellent for $\epsilon = 0.009$ and 0.041 if $\beta \approx 10^{-2}$; for $\epsilon = 0.08$, the error is no more than 20% (except for a datum obviously in error), still within the error of the measurements. If β were 2×10^{-2} , say, the overall agreement would greatly improve.

Hester and Sonin's experiments exhibited a linear dependence of the current on the potential; this is also in agreement with our theory since $j_{\infty} \sim \psi_p^{1/2}$ and $\bar{j}/j_{\infty} \sim \psi_p^{1/2}$. On the other hand, Bettenger and Chen's theory predicted $\bar{j} \sim \psi_p^{3/2}$.

Figure 7 presents a nondimensional half-width versus \hat{l}/M for the same conditions of Fig. 6, from both theory (full line, $\beta = 10^{-2}$, dashed line, $\beta = 10^{-3}$) and experiments. The half-width $\theta_{1/2}$ is not $\hat{\theta}_{1/2}$; it is defined in the same way of $\hat{\theta}_{1/2}$, except that now the peak is defined as the current in excess of that predicted for an infinite probe. $[\theta_{1/2}]_{BC}$ is the prediction from Bettenger and Chen's theory, for cold ions. The use of $\theta_{1/2}$ allows direct comparison with the experiments of Ref. 6. The agreement is, in general, good for $\beta \approx 10^{-2}$.

The experiments showed no dependence of $\hat{\theta}_{1/2}$ (or of $\theta_{1/2}$) on ψ_p ; this is also in complete agreement with our theory, as easily

verified in Eq. (65) (on the other hand the theory of Ref. 2 predicted $\theta_{1/2} \sim \psi_p^{-1/4}$). We also note that for cold ions, our theory predicts that $\theta_{1/2}$ is linear in ϵ ; this would explain the claim in Ref. 6 that the experimental data for $\theta_{1/2}/[\theta_{1/2}]_{BC}$ correlate in a single universal curve. However we point out that for many of the experimental points of Fig. 7, as in Fig. 6, the ions can not be considered as cold ($\eta > 0.5$). [Even for cold ions, all curves do not exactly meet except for small \hat{l}/M , because of logarithmic effects].

IV - Conclusions

The present paper deals with a significant end effect in the current response of a cylindrical Langmuir probe in a collisionless plasma flow. Infinitely-long probe theory predicts that when the angle θ between probe axis and flow direction decreases, the current experiences a smooth decrease; for a finite probe, however, the current may exhibit a strikingly different behavior, in the form of a strong peak at small θ . The peak, which may be substantial even for very long probes, appears when the potential is highly negative and both the ion-acoustic Mach number, M , and the ratio of Debye length to probe radius ϵ^{-1} are large.

The only analysis of this end effect available until now were a crude theory for the regime $\hat{l} > 3M$ (\hat{l} being the ratio of probe length to Debye length)³ and some numerical computations for $\hat{l} < 3M$ and $\theta = 0$.⁵ Here, the regime $\hat{l} < 3M$ is rigorously studied for θ arbitrary

within the peak region. The unperturbed ion distribution function is supposed to be Maxwellian. It is found that the nondimensional, average current density \bar{j}/j_∞ [where $j_\infty = \bar{j}(\hat{l} \rightarrow \infty)$] may be written as

$$\frac{\bar{j}}{j_\infty} = \frac{\bar{j}}{j_\infty} \left[\frac{\hat{l}}{M}, \epsilon, \beta, \psi_p, M\theta \right] \quad (66)$$

where β is the temperature ratio and $\psi_p = -eV_p/\kappa T_e$ (V_p being the probe potential and T_e the electron temperature). Specifically it is found that

$$\left[\frac{(8\psi_p)^{1/2} \hat{l}}{\pi \epsilon M \sigma^2} \right] \frac{\bar{j}}{j_\infty} = X(\mu, \eta, s) \quad (67)$$

where

$$\mu = \left[\frac{(\sigma^2 - 1)^{1/2} M}{(\psi_p \bar{\delta} \ln \sigma^2)^{1/2}} \right] \theta, \quad (68)$$

$$\eta = \frac{2\beta(\sigma^2 - 1)}{\psi_p \bar{\delta} \ln \sigma^2}, \quad (69)$$

$$s = 2 \frac{1 - \sigma^{-2}}{\ln \sigma^2}, \quad (70)$$

and

$$\bar{\delta}^{-1} = \ln \epsilon^{-1} + Y(\epsilon, \psi_p), \quad (71)$$

$$\sigma \operatorname{Erf} (\ln \sigma)^{1/2} = \frac{(2\psi_p \bar{\delta})^{1/2} \hat{l}/M}{\epsilon [\pi + 0.6 (\hat{l}/M)^2]^{1/2}}; \quad (72)$$

Y is given in Fig. 1. X is linear in s so that a single graph for $X(u)$ with two families of curves covers all conditions; this graph is given in Fig. 3. The brackets in Eqs. (67) and (68) are scaling factors so that Fig. 3 gives $[\bar{j}/j_\infty](\theta)$ directly. Explicit formulae are presented for the main features of the peak (its maximum and its half-width). All predictions of the theory agree well with experimental data.

The end effect may be advantageously used for diagnostic purposes. The first point to note is that the electron temperature has no effect on the peak; the dependence of \bar{j}/j_∞ on T_e cancels out except by way of $\bar{\delta}$; such dependence is very weak since the logarithmic variation in the term $\ln \epsilon^{-1}$ is substantially balanced by Y . Since j_∞ does not depend on T_e either, other aspects of probe response (usually the slope of the logarithm of the current for weakly negative potentials) must be used to determine the electron temperature.

Apart from parameters not related to the plasma (U , ℓ , r_p) and weak (logarithmic) effects, the maximum and the half-width of the peak can be written as

$$\left. \frac{\bar{j}}{j_\infty} \right|_{\max} = \left. \frac{\bar{j}}{j_\infty} \right|_{\max} \left[\frac{Z_1 N_0}{m_1}, \frac{Z_1 eV_p}{m_1}, \frac{\kappa T_1}{m_1} \right], \quad (73)$$

$$\hat{\theta}_{1/2} = \hat{\theta}_{1/2} \left[\frac{Z_1 N_0}{m_1}, \frac{\kappa T_1}{m_1} \right] \quad (74)$$

where the right-hand sides are explicitly known functions, N_0 is the

plasma density and Z_1 , m_1 and T_1 are the charge number, mass and temperature of the ions. If $j_\infty(\theta = 0)$ can be accurately extrapolated from experimental data at moderately small θ , then $j_\infty(\pi/2)$ and $j_\infty(0)$ jointly yield N_0 and $Z_1 eV_p/m_1$. Equations (73) and (74) then give

$$V_p, m_1/Z_1, T_1/Z_1 \quad .$$

If that extrapolation is not possible or $2\psi_p/M^2$ is large [$j_\infty(0) \approx j_\infty(\pi/2)$], some additional datum is necessary to find all four N_0 , V_p , m_1/Z_1 and T_1/Z_1 . If $\eta < 0.5$, however, $X \approx X(\eta = 0)$ and it is possible to find N_0 , V_p and m_1/Z_1 without determining T_1/Z_1 .

The present analysis is subject to a number of restrictions. It is mainly based on a theory recently developed for a closely related problem in transient probe response.⁶ The most substantial restriction on the validity of that theory is that one must have

$$\hat{l} < 3M \quad ;$$

additional restrictions are

$$\epsilon \ll 1 \quad , \quad \psi_p \gg 1 \quad , \quad 2\beta/\psi_p \bar{\delta} \ll 1 \quad .$$

The last inequalities, although used extensively to simplify the

analysis, are hardly restrictive however because the end effect is small if they are not satisfied. The use of the aforementioned transient probe theory in the present context is found to also require (approximately)

$$\psi_p < M^2 ,$$

$$\psi_p < \hat{\ell}^2 .$$

(Some additional conditions are discussed in the Appendix.)

ACKNOWLEDGMENTS

The author is highly grateful to Prof. A. A. Sonin for valuable discussions and suggestions.

This research was supported by the Advanced Research Projects Agency of the Department of Defense and was monitored by the Office of Naval Research under Contract No. N00014-0204-0040, ARPA Order No. 322.

Appendix

When the probe is not exactly aligned with the flow the ion density is not centrally symmetric because of the drift $U \sin \theta$. In Sec. II it was assumed that this asymmetry had no sensible effect on the ion current to the probe. The asymmetry shows up twice in the equation for the radial motion of an ion

$$\epsilon^2 \frac{d^2 \rho}{d\tau^2} = \frac{\partial \psi}{\partial \rho} + \frac{\epsilon^2}{\rho} \left[\lambda_0 + \epsilon^{-2} \int_0^\tau \frac{\partial \psi}{\partial \phi} d\tau' \right]^2 \quad (A1)$$

where λ_0 is the nondimensional angular momentum at time $\tau \equiv \omega_p t = 0$ (when the ion crosses the $z = 0$ plane) and the second term in the bracket represents the change in angular momentum due to the azimuthal field. When $\theta = 0$, we have $\partial \psi / \partial \phi = 0$ and it is possible to determine the region A^* and to find the function $\hat{a}^*(\tau)$ in Eq. (20) by using Eq. (16) in (A1). If $\theta \neq 0$, however, we have $\partial \psi / \partial \phi \neq 0$; $\partial \psi / \partial \rho$ now depends on ϕ and the second term in the bracket in (A1) does not vanish.

To get an estimate of the importance of the asymmetry, we first note that in the plane $z = 0$ the ion density is uniform. As z increases the ions readjust their distribution function. If the probe is sufficiently long the "infinite" (two-dimensional) limit density is finally reached. For simplicity of discussion we assume that the limit charge density can be written as

$$v_\infty = v_{c\infty} + v_{\phi\infty} \cos \phi \quad (A2)$$

where $v_{c\infty}$ and $v_{\phi\infty}$ are functions of ρ only. A (very) conservative estimate of $v_{\phi\infty}$ for $\rho < \rho_m$ would be $v_{\phi\infty} = 1$ [note that within the θ -range of interest, the peak, we have $\alpha_T < 1$ or $(M \sin \theta)^2 / 2\psi_p < \delta/2 \ll 1$]; for $\rho > \rho_m$ we may take $v_{\phi\infty} = 0$. If the probe is sufficiently short the asymmetry has no time to develop. A conservative estimate of the time required to reach the limit charge density (A2) would be an ion plasma period or $\hat{l} = 2\pi M$. The longest probes here considered have $\hat{l} \approx 3M$. Thus we consider $\hat{l} \approx 3M$ and assume

$$v_{\phi}(z = 0) = 0$$

$$v_{\phi}(z = l) = v_{\phi\infty} \cos \phi \frac{3}{2\pi}, \quad v_{\phi\infty} = 1,$$

and a linear growth from $v_{\phi}(z = 0)$ to $v_{\phi}(z = l)$. It is then possible to determine the ϕ -dependent part of ψ and its relative importance in Eq. (A1). We find that, under the worst conditions, the ϕ -dependence affects no result by more than 10%. Because of the conservative conditions used, this should justify our neglecting $\partial\psi/\partial\phi$ in Sec. II.

There is an assumption underlying the preceding discussion and the main body of our analysis that deserves consideration. This assumption is that the ion distribution function at $z = 0$ is the unperturbed distribution function far ahead of the probe. Obviously the field ahead of the probe tip will somehow affect the ions reaching

the plane $z = 0$. Since $\epsilon \ll 1$ and the potential field around the tip should be roughly spherically symmetric, we can assume this field to be $\psi \approx \psi_p/\rho$, (in order to get a rough estimate of the importance of that effect). Then the ion motion for $z < 0$ can be solved exactly; we find, for instance, that

$$\frac{z_1 N_1}{N_0} (z = 0) = 1 + \frac{W^2}{1 + 2W} ,$$

$$2W = (1 + 2\psi/M^2)^{1/2} - 1 .$$

It may be shown that the perturbations in ion density and ion azimuthal velocity are of no importance. The perturbation in ion radial velocity, however, may in some cases be so large as to affect the ion current to the probe. This occurs when the probe is very short ($\hat{\ell} \ll 3M$) and ψ_p/M^2 is close to unity [remember condition (44)].

Finally, since our entire analysis is restricted to the regime $\hat{\ell} < 3M$, we would like to comment briefly on Bettinger and Chen's theory for the regime $\hat{\ell} > 3M$.³ To well understand point (D) below, we emphasize here that the limitation $\hat{\ell} < 3M$ of our analysis originates from our lack of a good approximation for $\partial\psi/\partial\rho$, for $\rho > \rho_m$; such values of ρ come into play when $\hat{\ell} > 3M$. When $\partial\psi/\partial\rho$ is unknown $\hat{a}^*(\tau)$, and thus \bar{j}/j_∞ , cannot be determined.

In the light of our theory and of Fig. 2, Bettinger and Chen's approach may be resumed as follows: (A) they divided region A* in

two subregions, call them A_1 and A_0 , lying inside and outside the sheath, respectively. For the sheath radius [equivalent to our ρ_m or $\exp(\delta^{-1})$] they used an expression "a" patched up from numerical results for probes in quiescent plasmas. As pointed out in Ref. 5, "a" has a wrong dependence on ψ_p ; this leads to the wrong dependence of \bar{j} and $\theta_{1/2}$ on ψ_p indicated in Sec. III. (B) They assumed that all ions in A_1 are collected; this leads to the requirement $\hat{\ell} > \tau_m M \approx 3M$. For A_0 , they noticed that the appropriate equivalent time (probe length) was not $\tau_\ell \equiv \hat{\ell}/M$ but $\tau_\ell - \tau_m$. (They did not incorporate, however, this correction to their formulae; instead, in a comparison to some experiments, they adjusted appropriately the experimental data. This may lead to confusion: In the resume of Bettinger and Chen's theory given in Ref. 5, the correction was not considered; it may be easily verified that with such correction the overall agreement in Figs. 5a, b, c of Ref. 5 would improve). (C) To compute τ_m , power laws for $\partial\psi/\partial\rho$ were used instead of the correct expression given by Eq. 16. The variation of τ_m with the particular power law is not greatly significant however. (D) The most crucial point of their analysis is that for \hat{a}^* inside A_1 they wrote

$$\hat{a}_1^*(\tau) \sim (\tau_\ell - \tau_m)$$

where the proportionality constant is obtained from the limit $\tau_\ell \rightarrow \infty$. This is obviously wrong because the value of ψ at the sheath boundary

is still $O(1)$ so that for some distance outside the sheath, ion velocities are not well approximated by their asymptotic values, unless $\beta \gg 1$.

(This point is related to the well known Bohm's sheath criterion.) For $\beta \ll 1$ the error can be substantial except if τ_ℓ is very large. (E) A final error is the approximation of $\bar{\rho}_A(\phi)$ everywhere by its asymptotic value. The approximation is good for A_0 but not for A_1 . Thus, the resulting error should be noticeable for moderate τ_ℓ .

Nevertheless, on the whole, the agreement of the theory of Ref. 3 with experiment is good for moderate potentials. Thus, it should be possible to use that theory for $\hat{\ell} > 3M$, provided that an appropriate sheath radius (ρ_m) be used and the correction $\tau_\ell \rightarrow \tau_\ell - \tau_m$ be incorporated into the formulae.

References

1. J. G. Laframboise, University of Toronto Institute for Aerospace Studies Report No. 100 (1966).
2. H. M. Mott-Smith and I. Langmuir, Phys. Rev. 28, 727 (1926).
3. R. T. Bettinger and A. A. Chen, J. Geophys. Res. 73, 2513 (1968).
4. S. D. Hester and A. A. Sonin, in Rarefied Gas Dynamics, L. Trilling and H. Wachman, Eds. (Academic Press Inc., New York, 1969), Vol. II, p. 1659.
5. S. D. Hester and A. A. Sonin, Phys. Fluids 13, 1265 (1970).
6. J. R. Sanmartin, submitted to Phys. Fluids.
7. The second boundary of A^* in Fig. 2, $\bar{\rho}_A(\phi)$, excludes those ions below $\bar{\rho}_A(\phi)$ which initially move away from the probe ($\phi_0 > \pi/2$) and never turn back. This boundary plays no role here because ions initially at that boundary have a time of flight to the probe larger than t_m .

BLANK PAGE

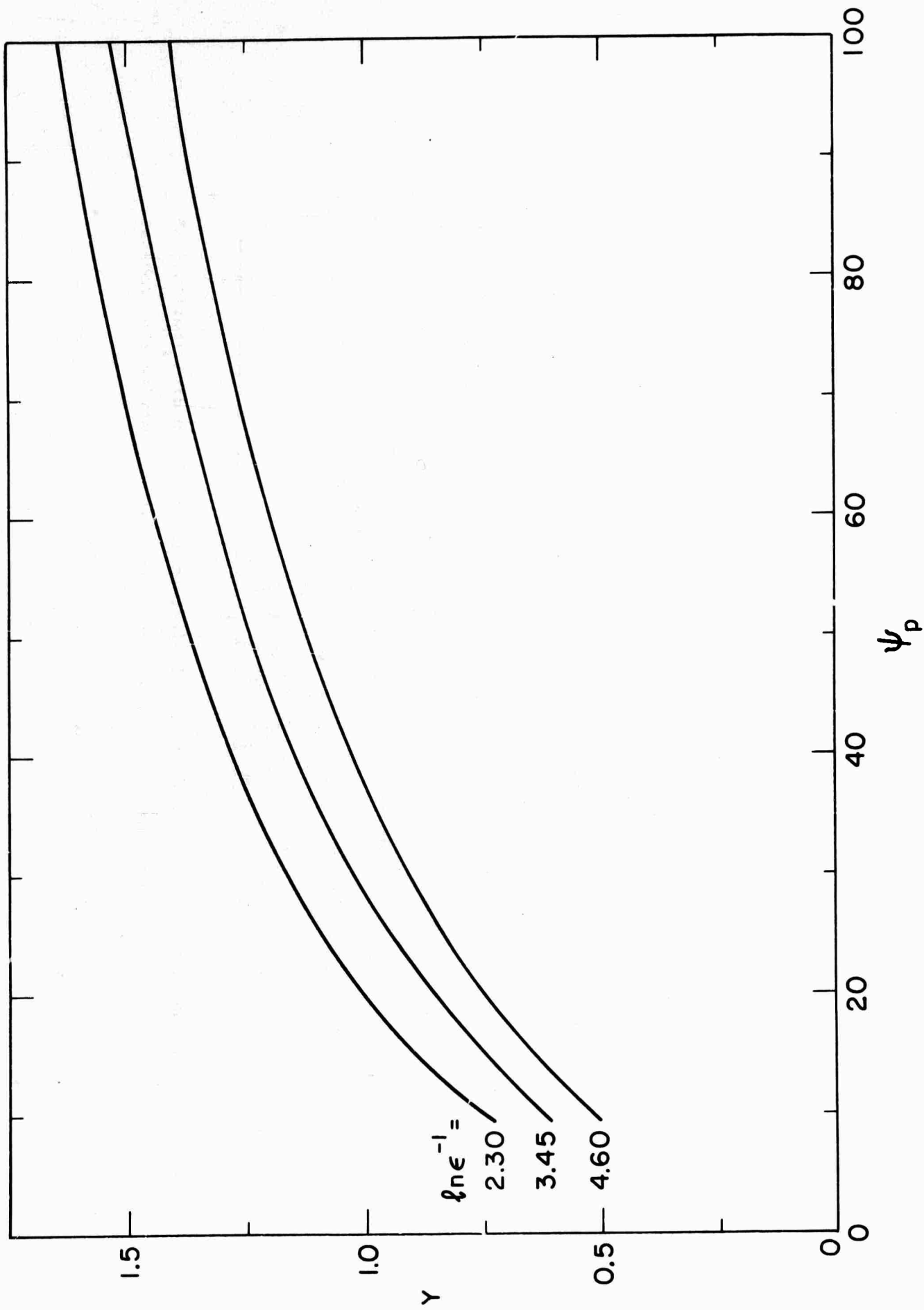


Fig. 1 Auxiliary function Y vs. ψ_p and ϵ .

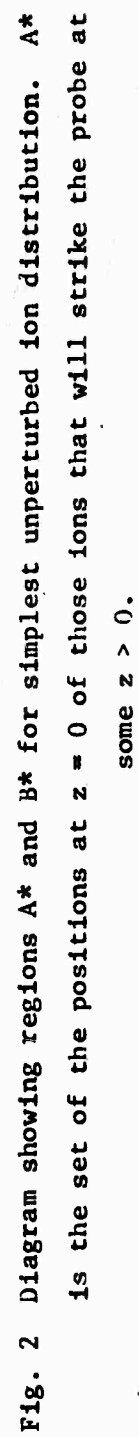


Fig. 2 Diagram showing regions A* and B* for simplest unperturbed ion distribution. A* is the set of the positions at $z = 0$ of those ions that will strike the probe at some $z > 0$.

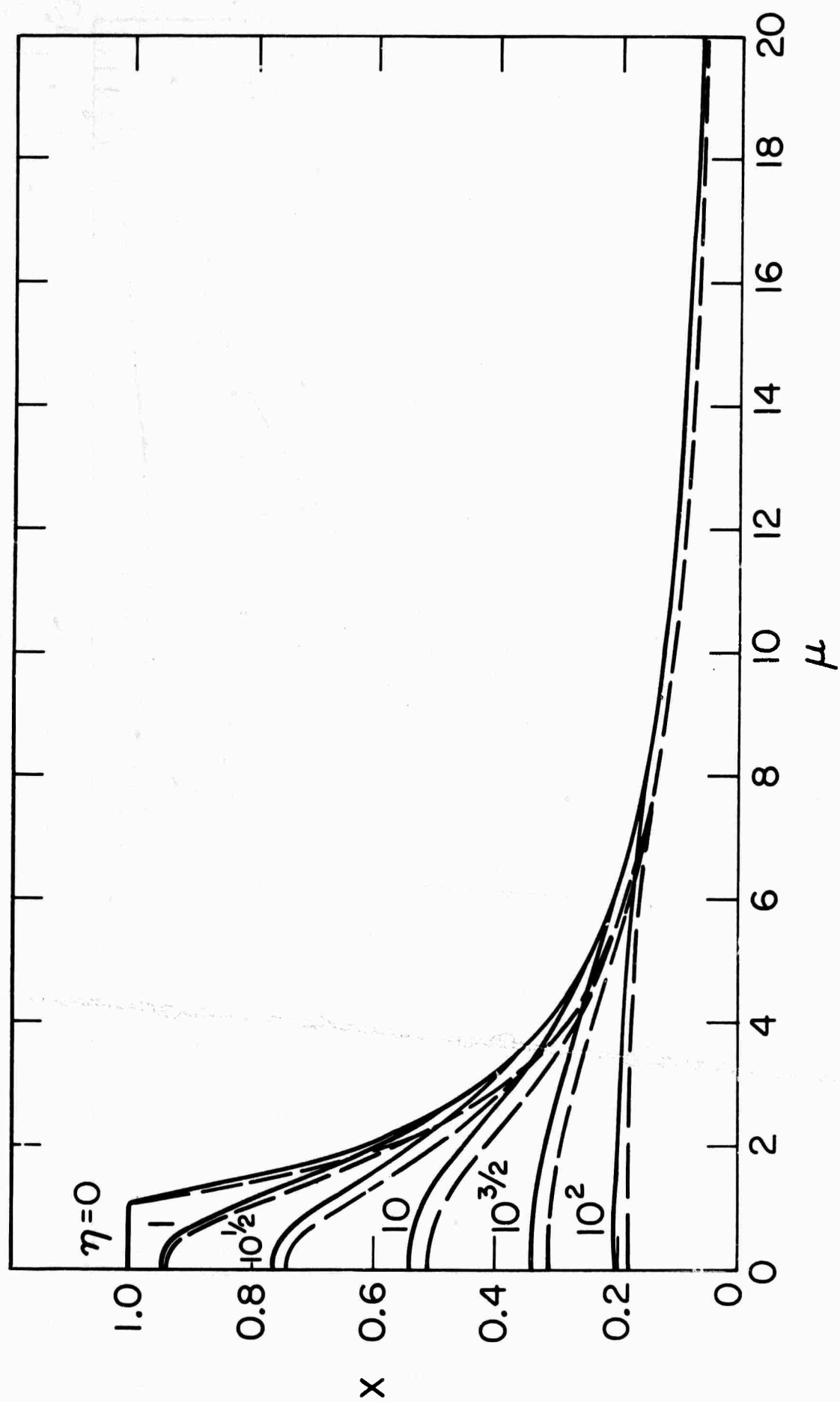


Fig. 3 Angular dependence of current peak.

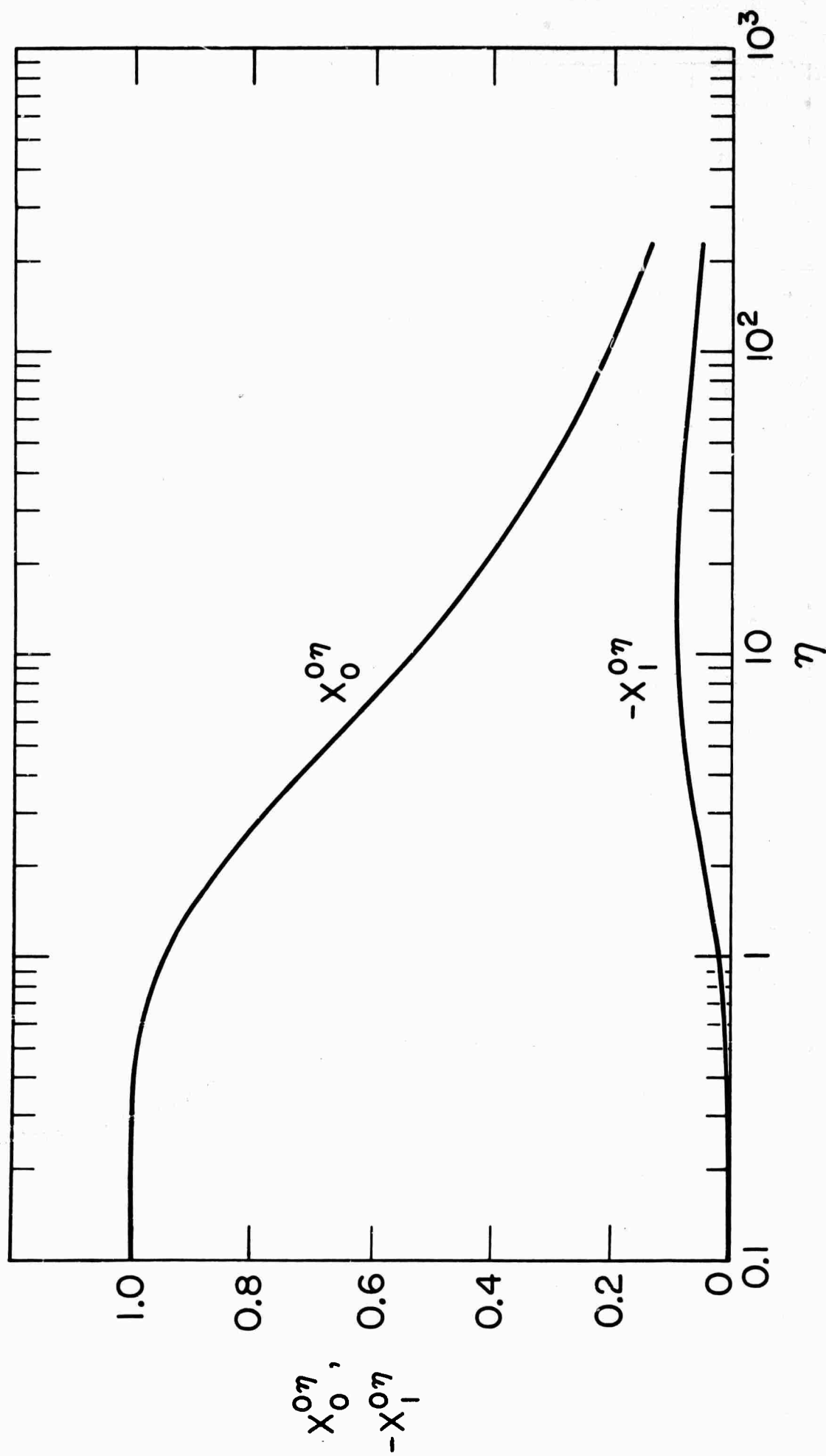


Fig. 4 Auxiliary functions for determination of maximum current ($\theta = 0$).

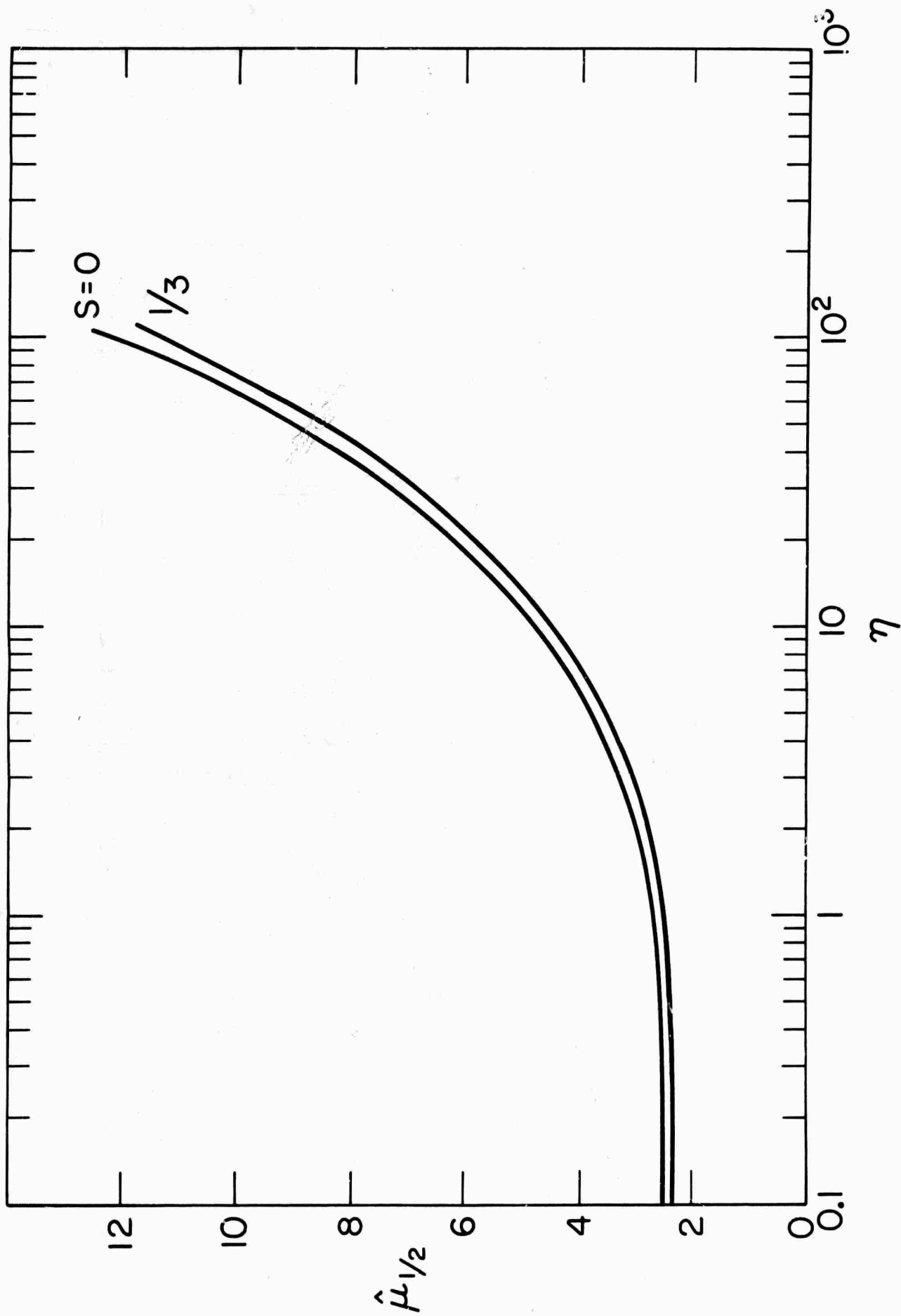


Fig. 5 Angular half-width of current peak.

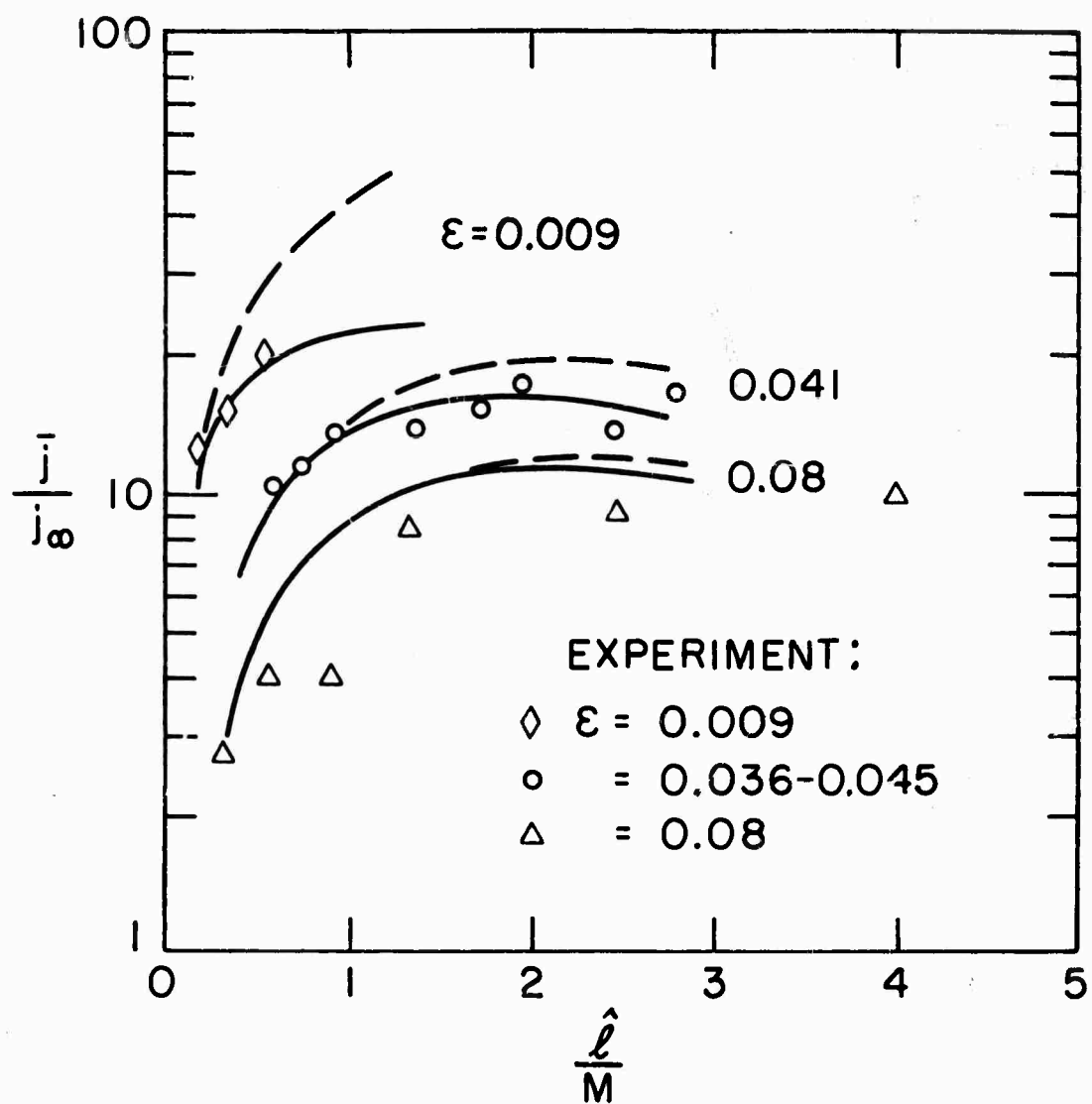


Fig. 6 Comparison of maximum current density ($\theta = 0$) from experiments (Ref. 5) and present theory (full lines $\beta = 10^{-2}$, dashed lines $\beta = 10^{-3}$).

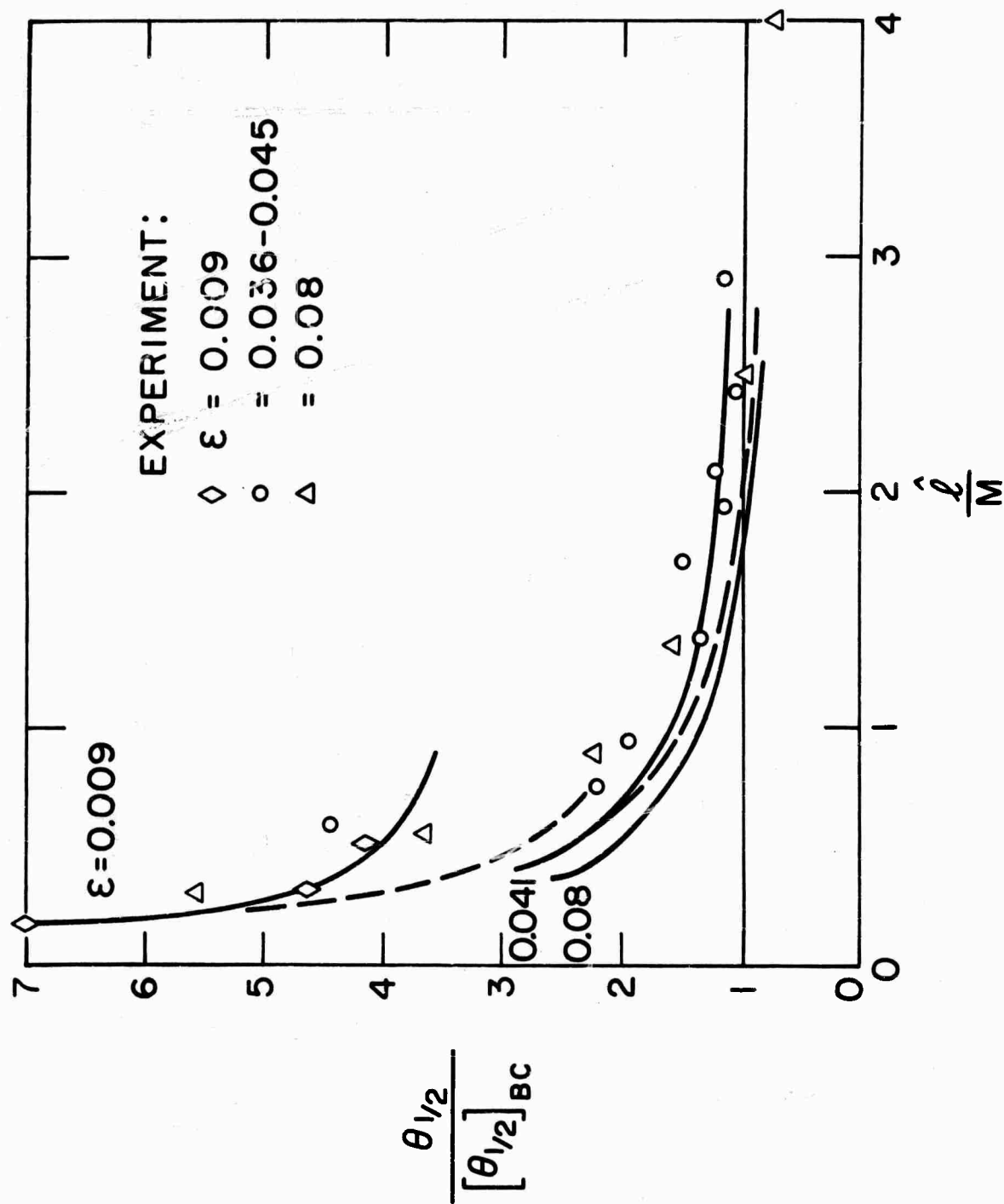


Fig. 7 Comparison of angular half-width (as defined in Ref. 5) from experiments (Ref. 5) and present theory (full lines $\beta = 10^{-2}$, dashed lines $\beta = 10^{-3}$).